

The Arabidopsis AtbZIP9 protein fused to the VP16 transcriptional activation domain alters leaf and vascular development

Amanda Bortolini Silveira^{a,1}, Luciane Gauer^{a,1}, Juarez Pires Tomaz^a,
Poliana Ramos Cardoso^b, Sandra Carmello-Guerreiro^b, Michel Vincentz^{a,c,*}

^aCentro de Biologia Molecular e Engenharia Genética, Universidade Estadual de Campinas, Cidade Universitária “Zeferino Vaz”,
Distrito de Barão Geraldo 13083875, CP6010, Campinas, SP, Brazil

^bDepartamento de Botânica, Instituto de Biologia, Cidade Universitária “Zeferino Vaz”, Distrito de Barão Geraldo 13083970, CP6109, SP, Brazil

^cDepartamento de Genética e Evolução, Instituto de Biologia, Cidade Universitária “Zeferino Vaz”,
Distrito de Barão Geraldo 13083970, CP6109, SP, Brazil

Received 8 December 2006; received in revised form 28 February 2007; accepted 5 March 2007

Available online 14 March 2007

Abstract

The Arabidopsis group C bZIP transcriptional regulatory factors includes four members that are homologous to the maize *Opaque-2* regulatory locus. These four Arabidopsis bZIP were organized into three groups of orthologues each of which possibly representing an ancestral angiosperm function. To better define the evolution of group C functions we initiated the characterization of *AtbZIP9*, a single Arabidopsis gene corresponding to one of the three group C ancestral functions and for which little functional information is available. Promoter fusion with GUS revealed that *AtbZIP9* expression is restricted to the phloem of all organs analyzed and *in situ* hybridization confirmed this conclusion. *AtbZIP9* mRNA accumulation was also shown to be repressed by glucose and induced by abscisic acid and cytokinin. *Knockout* T-DNA mutant or transgenic lines overexpressing *AtbZIP9* mRNA were undistinguishable from the wild type indicating that post-transcriptional regulation and/or genetic redundancy act on *AtbZIP9*. To overcome the redundancy aspect, we produced transgenic plants expressing a fusion between *AtbZIP9* cDNA and the VP16 transcriptional activator domain. These plants displayed leaf developmental defects and accumulation of phenolic compounds in the mesophyll. These alterations may be the consequence of changes in the phloem developmental process.

© 2007 Elsevier Ireland Ltd. All rights reserved.

Keywords: *Arabidopsis thaliana*; *AtbZIP9* transcription factor; VP16; Vascular cylinder development; Phloem

1. Introduction

The *Arabidopsis thaliana* (*Arabidopsis*) genome codes for 75 bZIP transcriptional regulatory factors which are organized into 10 groups of homologues [1]. Group C includes four genes (*AtBZIP10/Bzo2h1*; *AtbZIP9/Bzo2h2*; *AtbZIP63/Bzo2h3* and *AtbZIP25/Bzo2h4*) that are homologous to the maize *Opaque-2* (*O2*) locus [1,2]. *O2* expression is restricted to the developing endosperm where it controls storage protein gene expression and the carbon to nitrogen balance [3,4]. To which extent *O2*-

related function is conserved among eudicotyledonous species is still unclear. Detailed phylogenetic analysis indicate that the four group C genes possibly represent three groups of orthologues (i.e., ancestral angiosperm functions). *AtbZIP63*, which is likely the *O2* orthologue [2], is poorly expressed in seeds [5] and little is known about its function [5,6]. However, *BZI-1*, the probable tobacco orthologue of *O2* and *AtbZIP63*, was found to regulate and interact with an auxin-responsive promoter indicating a role in auxin signaling [7]. Moreover, tobacco plants expressing a dominant negative form of *BZI-1* which lacks the N-terminal sequence were shown to be more susceptible to tobacco mosaic virus infection, suggesting an involvement of *BZI-1* in pathogen response [8].

The second group of orthologues within group C is represented by the two paralogous genes *AtbZIP10* and *AtbZIP25*. The corresponding bZIP factors were shown to interact with the regulatory factor *ABI3* to control the activity

* Corresponding author at: Centro de Biologia Molecular e Engenharia Genética, Universidade Estadual de Campinas, Cidade Universitária “Zeferino Vaz”, Distrito de Barão Geraldo 13085970, CP6010, Campinas, SP, Brazil. Tel.: +55 19 35211140; fax: +55 19 35211089.

E-mail address: mgavince@unicamp.br (M. Vincentz).

¹ These two authors contributed equally to this work.

of the *At2S1* albumin gene promoter [5]. AtbZIP10 and AtbZIP25 may therefore be functionally more related to O2 than AtbZIP63. Surprisingly, AtbZIP10 was found to act as a positive regulator of hypersensitive response and basal defense processes, and LSD1 inhibits its activity by a cytoplasmic retention regulatory step [6]. In addition, AtbZIP10 is involved in the control of proline metabolism. Indeed, it was shown that AtbZIP10 can form heterodimers with AtbZIP53 (a member of the group S of homologues [1]) to activate the transcription of the proline dehydrogenase gene [9]. This later finding is quite relevant since a network of specific heterodimerization between group C and group S bZIP factors has been described and this pattern of interaction may play an important role in the modulation of the activity of the C/S bZIPs [10].

The third group of orthologues which is more distantly related to O2 [2], includes *AtbZIP9* and functional data are still lacking for this gene. To gain more insight into the functional evolution of group C bZIP proteins, we initiated a detailed characterization of *AtbZIP9*. Here, we present evidence that the expression of a fusion between the VP16 and AtbZIP9 induces significant changes in leaf development and in the structure of the vascular bundle.

2. Materials and methods

2.1. Plant material and growth conditions

Arabidopsis thaliana Columbia-0 (Col-0) or Wassilewskija (Ws) ecotypes, were grown on a mixture of soil and vermiculite (2/1) or *in vitro* on solid half-strength Murashige and Skoog medium (MS/2; SIGMA) [11] containing 0.5% sucrose under a 16-h light:8-h dark cycle at 22 °C. For *in vitro* growth, seeds were surface sterilized and incubated for 3 days at 4 °C in the dark to break dormancy. Seeds of *atbzip9-1* T-DNA knockout (insertion in exon 5 of *At5g24800*; Fig. 3A) null mutant were obtained from Syngenta (Arabidopsis Insertion Library, Access number 569C12 [12]). Seedlings of the *abi5-1* (Ws) mutant expressing a HA-ABI5 fusion protein were described earlier [13]. Seedlings were selected *in vitro* with 100 µg kanamycin/ml and transgenic individuals were transplanted on kanamycin-free medium 4 days after germination. For the ProAtbZIP9-GUS and 35S-AtbZIP9 constructs (described hereafter), homozygotic lines for one locus were selected by analysis of kanamycin resistance segregation. For expression analysis, surface sterilized seeds were sown in liquid MS/2 medium without carbon source for 5 days under constant dim light and under slow agitation (67 rpm). Seedlings were then exposed to 2% glucose (w/v) or 100 µM ABA or 50 µM cytokinin for 4 and 24 h.

2.2. DNA constructs

Translational fusion between the *AtbZIP9* promoter and the reporter gene *gusA* was obtained as follows. The *gusA* coding sequence followed by the *Nos* gene poly(A) signal was obtained from pBI121 [14] as a *HindIII/EcoRI* fragment which was cloned into pUC18 [15] to form *gusA*-poly(A)-pUC18 plasmid.

The *AtbZIP9* (*At5g24800*) promoter sequence (2000 bp upstream of the start codon) and 52 bp of N-terminal coding sequence were amplified with the two primers CTTTAACCTG-CAGCTTCAATCTCGTTCACG and CCAGCTCGGATCCACCTTCTCTCCATGGCAATGTC and the resulting fragment was cloned into pGEMT-Easy (Promega). Subsequently, the promoter sequence was inserted in frame with *gusA* by ligation into the *PstI* and *BamHI* sites of *gusA*-poly(A)-pUC18 to generate ProAtbZIP9-GUS. ProAtbZIP9-GUS was introduced into the binary vector pCAMBIA 2300 (www.cambia.org) using the *PstI-EcoRI* sites. *AtbZIP9* superexpressor allele was assembled starting with the *AtbZIP9* complete cDNA (AF310223). A 851 bp *Hind-EcoRI* fragment corresponding to the full-length cDNA cloned in pUC18 was treated with DNA polymerase I large (Klenow) fragment (Invitrogen) and cloned in pRT-Ω vector, digested with *BamHI* and blunt-ended with Klenow, between the CaMV 35S promoter and its poly(A) signal [16]. The resulting construct was designated 35S-AtbZIP9 and was introduced into the *PstI* site of the binary vector pCAMBIA 3300 (www.cambia.org). An *AtbZIP9* dominant activator allele was constructed by obtaining in a first step a promoter sequence which excludes any coding sequence. To this end, 484 bp upstream of the start codon of the promoter 3' end sequence was amplified with the two primers CGAAATATTTAGGATCCTTTTATG and TTCTTTGAATG-TCTAGACACAAGA. This amplification product was ligated to the remaining promoter 5' end to reconstitute a full-length 1972 bp *AtbZIP9* promoter that was cloned in *PstI* and *XbaI* sites of pBKS [17]. The CaMV 35S promoter in pRT100 [16] was replaced by the *AtbZIP9* promoter using *XhoI-XbaI* digestion producing the plasmid PAtbZIP9. The *AtbZIP9* coding sequence was amplified from the cDNA (AF310223) with the two primers GCCAGTGCCGAGCTCCAAA-GAAAATGG and CCATGATTACGGATCCGAGTCATGGC and the resulting product was inserted into the *SstI-BamHI* sites of PRT100 to obtain the cDNAAtbZIP9 plasmid. A triple hemagglutinin (HA) tag and the *Herpes simplex* virus VP16 activation domain were amplified from the PFP101-HA-VP16 vector [13] with the two primers CCCCCCTCTA-GAAAAAATGGCATACCCATACGAC and GACTTGGATGAGCTCTAGTGATATCCC and cloned into *XbaI-SstI* sites of pBKS. After digestion with *XhoI-SstI* the HA-VP16 fragment was fused in frame to the 5' end of cDNAAtbZIP9, generating HA-VP16::cDNAAtbZIP9. This latest construct was then digested with *XbaI* to release the HA::VP16::cDNAAtbZIP9 fusion which was cloned downstream of the *AtbZIP9* promoter in the PAtbZIP9 plasmid. The expression cassette *AtbZIP9* promoter::HA-VP16::cDNAAtbZIP9::poly(A), designated VP16-AtbZIP9 was excised with *PstI* and introduced into the binary vector pCAMBIA2300. All amplification fragments were verified by sequencing.

2.3. Plant transformation

Agrobacterium-mediated plant transformation was realized basically according to the *in planta* transformation protocol described by Bechtold [18]. *Agrobacterium tumefaciens*

(GV3101::pMP90 [19]) carrying the binary vector with the constructs of interest was sprayed over plants just before bolting. The chimeric genes 35S-AtbZIP9 and ProAtbZIP9-GUS were transferred into wild type (Col-0 ecotype), while the VP16-AtbZIP9 construct and the VP16 transcriptional activator domain under the control of the CaMV 35S promoter in the pFP100 vector [13] were transferred into *atbzip9-1* T-DNA insertion line.

2.4. RNA isolation, reverse transcription and PCR

Total RNA was extracted in Guanidine HCl 8 M (Invitrogen), Tris HCl pH 8.0 50 mM (Invitrogen), EDTA pH 8.0 20 mM (Invitrogen) and 50 mM β -mercaptoethanol as described by Logemann et al. [20]. Total RNA were denatured and subsequently fractionated by electrophoresis in denaturing 5% formaldehyde, 1% (w/v) agarose gel according to Logemann et al. [20]. Six micrograms of total RNA were reverse transcribed in a 50 μ L reaction volume using ImProm II Reverse Transcriptase (Promega) and oligodT18 oligonucleotide (Invitrogen) according to the manufacturer's instructions. PCR was carried out using 5 μ l of the cDNA with 1.5 U of Taq polymerase (Invitrogen) in a 50 μ l reaction. Amplifications were performed with the following steps: 94 °C for 3 min; cycles of 94 °C for 45 s, 60 °C for 30 s and 72 °C for 90 s; ending with a final extension of 72 °C for 5 min. *Actin2* (At3g18780) and adenosine phosphoribosyl transferase *Apt1* (At1g27450) genes were used as endogenous controls for

standardization of the cDNA amount. *Actin2* was amplified with CGTACAACCGGTATTGTGCTGG and AACGATTCCTG-GACCTGCCTCATC primers and *Apt1* with TCCCA-GAATCGCTAAGATTGC and CCTTCCCTTAAGCTCTG primers. *AtbZIP9* mRNA (At5g24800) was amplified using CAAGCCCTCTAGACCCTTG and GATGTCTGAGACG-CAGCTAAC primers. *β -Amilase* (At4g17090), *ABI5* (At5g52310) and putative cytokinin response regulator (*Arr15*; At1g74890) were used as control genes for induction by glucose, ABA and cytokinin treatment, respectively. *β -Amilase* was amplified with GCTACGACAAGTATAT-GAAATCG and CCACATTCTCAGCGATCTTGCC primers; *ABI5* with CTTGAGGATTTCTTGGTGAAG and CACTGTA-TATGCTTGTTC primers and *Arr15* with CGTATAGAA-CAATGTATGATAG and CCCCTAGACTCTAATTTGATC primers.

2.5. Western blot analysis

For total protein extraction, 600–800 mg of fresh plant material was ground to a fine powder in liquid nitrogen and homogenized in 1 ml of extraction buffer (Tris HCl pH 8.5 50 mM, EDTA pH 8.0 2 mM, dithiothreitol 5 mM, NaCl 50 mM, triton X-100 0.1%, Leupeptin 100 μ M and PepstatinA 2 μ M). After 20 min centrifugation at 13000 rpm and 4 °C, the supernatant was saved and protein concentration was determined using BioRAD Protein Assay (Bio-Rad) following the manufacturer's instructions. Protein extracts diluted 1:1 in

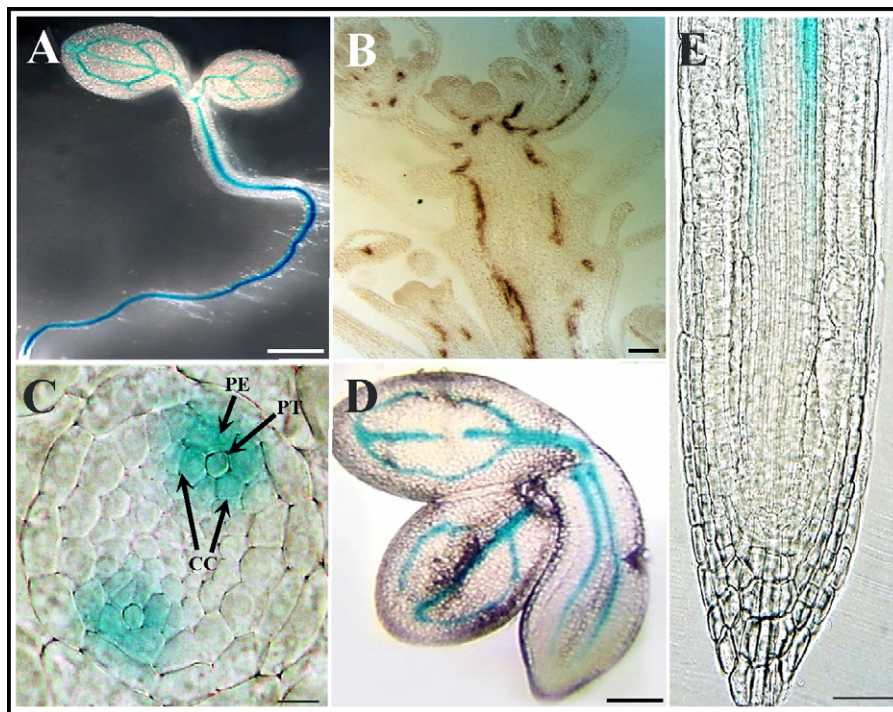


Fig. 1. Expression of *AtbZIP9*. (A, C, D, E) *In situ* localization of ProAtbZIP9-GUS expression. GUS activity was located in vascular tissue. (A) Early stages of vegetative growth, 3 days after germination. (B) *In situ* localization of *AtbZIP9* mRNA, cross-section through a wild-type floral meristem indicated mRNA accumulation in vascular bundle. (C) Transverse section through primary root showed GUS specific expression in phloem and pericycle cells at the phloem pole. (D) Mature embryo, GUS activity was found in undifferentiated procambium cells. (E) Longitudinal section through primary root showed GUS expression in root vascular cylinder differentiation and elongation meristematic zone. PE, pericycle; PT, protophloem; CC, companion cells. Scale bars: (A) 700 μ M; (B) 65 μ M; (C) 10 μ M; (D) 80 μ M; (E) 50 μ M.

loading buffer (Tris HCl 125 mM pH 6.8, dodecyl sodium sulfate 4%, β -mercaptoethanol 10%, glycerol 20% and bromophenol blue 0.04%) were denatured, resolved by electrophoresis on 10% SDS-polyacrylamide gel (PAGE) and subsequently blotted onto Hybond ECL 0.45 μ m nitrocellulose membranes (Amersham Biosciences). The primary antibody (Rat anti-HA High Affinity 3F10, Roche Applied Science) diluted 1/1000 and the secondary antibody (ECL anti-rat IgG Horseradish peroxidase-Linked, NA935, Amersham Biosciences) diluted 1/10000 in Tris-buffered saline (TBS), 0.1% Tween 20, 5% skimmed milk, were successively incubated with the membranes at room temperature for 10 and 2 h, respectively. Amersham ECL PlusTM Western Blotting Detection Reagents were used for revelation following manufacturer's recommendation.

2.6. Histochemical assay of β -glucuronidase activity

GUS activity was detected *in situ* according to Jefferson [14]. Samples were fixed in 80% acetone for 1 h at -20°C and subsequently incubated in GUS reaction buffer (sodium phosphate buffer 100 mM pH 7, 10 mM EDTA, 0.1% triton X-100 and 0.5 mM potassium ferrocyanide) containing 0.5 mg

X-gluc (3-indolyl-b-D-glucuronic acid; USB)/ml. Incubation was performed at 37°C in the dark, for different time periods according to the intensity of blue staining. Samples were chlorophyll depleted in 70% ethanol and stored at 4°C . The material was viewed using a Zeiss Stemi SV6 stereomicroscope. Images were acquired using digital Camera Canon Power Shot A95 and processed using Adobe Photoshop 6.0.

2.7. Cytological techniques and microscopy

For anatomical studies fresh tissues or GUS-stained samples were fixed for 24 h in FAA (formalin:acetic acid:50% ethyl alcohol = 5:5:90 v/v/v), dehydrated in a gradual ethanol series (50%; 70% and 100%), embedded in Historesin (glycol methacrylate, Leica, Heidelberg, Germany) according to manufacturer's instructions and sectioned with a Leica RM2245 microtome. Sections (8–10 μ m) were dried onto slides at 37°C and, if required, stained with toluidine blue. Phenolic compounds were detected using 10% (w/v) ferric chloride for 30 min. Samples were viewed using Leica DMI4000B microscopy. Images were acquired with Leica DFC300 FX Digital Camera System and processed using Adobe Photoshop 6.0.

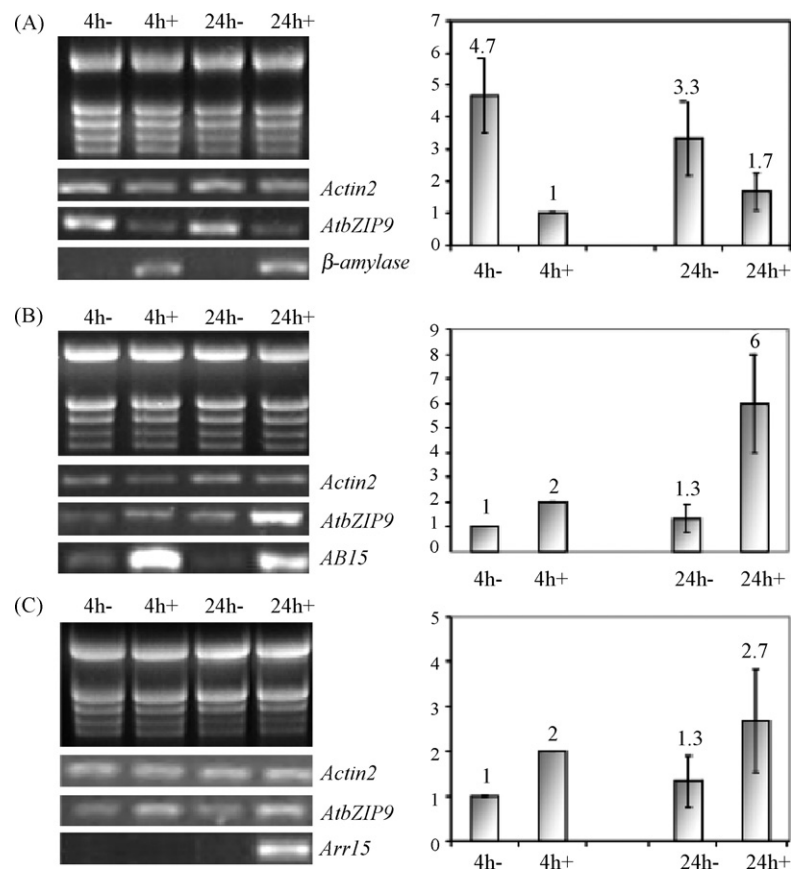


Fig. 2. Regulation of *AtbZIP9* expression. Five days old seedlings grown on liquid half-strength Murashine and Skoog medium were exposed to 2% glucose (A); 100 μ M ABA (B) and 50 μ M cytokinin (C) for 4 (4h+) and 24 h (24h+). For each treatment, untreated controls were obtained (4h-; 24h-). Integrity of total RNA (3 μ g) was verified by denaturing agarose gel analysis (left row upper part in A, B and C). RT-PCR products of *AtbZIP9*, *Actin2*, and treatment-control genes, β -*amilase* for glucose treatment, *ABI5* for ABA treatment and *Arr15* for cytokinin treatment are shown. *Actin2* was used as control for normalization of cDNA amount. The linear phase of the exponential PCR reaction was corroborated for each gene (data not shown). For each treatment, a relative quantification was realized by serial dilutions of the PCR products and the means of three experiments are shown in the graphics on the right (bars represent standard deviation of the mean).

2.8. *In situ* mRNA localization

Influorescences were fixed in 4% *p*-formaldehyde, 10 mM dithiothreitol, 1× PBS buffer for 16 h. The material was dehydrated, infiltrated and parafin-embedded. T7 polymerase and DIG were used for digoxigenin-labelled antisense and sense riboprobes synthesis according to manufacturer's instructions (Boehringer Mannheim). Sections (8–10 μM) were hybridized with antisense and sense RNA probes. Sense and antisense RNA probes were made using the entire 855 bp cDNA (Access number AF310223) cloned into *Hind*III-*Eco*RI sites of pUC18 and pBKS.

3. Results and discussion

3.1. Expression of *AtbZIP9*

Six independent transgenic lines homozygous for the Pro*AtbZIP9*-GUS construct inserted at one locus showed a consistent expression pattern of GUS restricted to the vascular system of all organs: roots, hypocotyl, cotyledon, leaves, flowers and siliques (Fig. 1A and results not shown). *In situ* mRNA hybridization showed that the *AtbZIP9* mRNA accumulated in the central vasculature region (Fig. 1B) indicating that the promoter sequence was sufficient to reproduce the *in vivo* *AtbZIP9* mRNA expression profile. In roots, GUS activity was detected in phloem and pericycle cells at the phloem pole, defining a bilateral symmetry (Fig. 1C). In addition, GUS expression was also evident in the differentiation and elongation meristematic zone of the root vascular cylinder (Fig. 1E), suggesting that *AtbZIP9* possibly has a role in phloem development. This observation is consistent with the presence of β-glucuronidase activity in undifferentiated procambium cells of maturing embryos (Fig. 1D). Gus activity was also detected in the phloem of leaves and inflorescence stem (data not shown). Phloem expression of *AtbZIP9* described here is in agreement with recent Arabidopsis phloem transcriptome data [21] and *in situ* detection of *AtbZIP9*-GFP fusions [22]. The regulation of *AtbZIP9* expression in response to different hormones was investigated. Auxin, ethylene, gibberellic acid and jasmonic acid did not alter *AtbZIP9* mRNA abundance. However, we showed that during a 4-h interval, *AtbZIP9* expression was repressed by glucose and induced by abscisic acid (ABA) and cytokinin (Fig. 2). Based on these data, we suggest that *AtbZIP9* could possibly participate in glucose, ABA and cytokinin signaling to control some aspect of development and/or physiology of the phloem.

3.2. Changing the expression level of *AtbZIP9* does not affect plant development

To further investigate the function of *AtbZIP9*, we analyzed a T-DNA insertion *knockout* null mutant (*atbzip9-1*, Fig. 3A) and a transgenic line overexpressing the *AtbZIP9* mRNA from the CaMV 35S promoter (35S-*AtbZIP9*) (Fig. 3B). Comparative analysis of growth and development under standard conditions did not reveal any detectable phenotypic difference

between the *atbzip9-1* null mutant, 35S-*AtbZIP9* and wild-type plants (Fig. 3C). Alterations of the nitrogen or carbon supply, dark/light regime and temperature stresses also failed to reveal any clear effect of *AtbZIP9* on Arabidopsis life cycle. Based on its expression pattern we suggest that *AtbZIP9* could be involved in phloem development. This prompted us to perform a comparative analysis of root vascular system anatomy between *atbzip9-1 knockout* mutant, 35S-*AtbZIP9* and wild-type plants. Root vascular cylinder structure was found to be quite similar in the three genotypes (Fig. 3D), suggesting that *AtbZIP9* is apparently not essential for phloem development. The lack of any clear effect of overexpressing *AtbZIP9* mRNA on plant development may be interpreted as reflecting post-transcriptional regulation of *AtbZIP9* gene expression. Moreover, the lack of impact of *AtbZIP9* null allele on plant development may be a consequence of functional redundancy among members of group C bZIPs. The presence of GUS activity in the vascular cylinder of *AtbZIP10* and *AtbZIP63* promoter Gus reporter lines (data not shown) is consistent with this hypothesis.

3.3. The *VP16-AtbZIP9* fusion protein promotes alteration of leaf and vascular strand development

In order to overcome the possible redundancy existing among group C bZIPs [23], and to obtain functional cues for

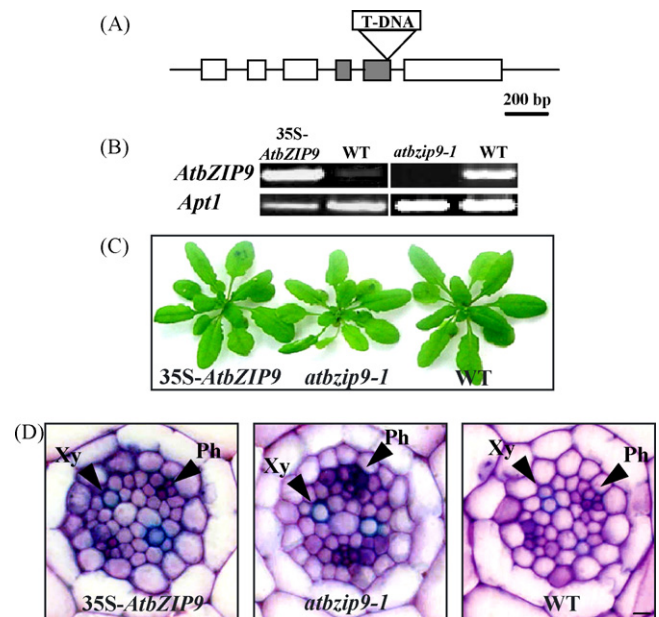


Fig. 3. Characterization of transgenic plants expressing different levels of *AtbZIP9*. (A) Schematic representation of the exon–intron structure of the *AtbZIP9* gene. Boxes represent exons, lines introns and gray boxes indicate the exons encoding the bZIP DNA-binding domain of *AtbZIP9*. The T-DNA is inserted at the end of *AtbZIP9* exon 5 (Syngenta line 569C12). The T-DNA insert is not drawn to scale. (B) Semi-quantitative RT-PCR analysis of *AtbZIP9* gene expression in transgenic plants homozygous for one locus of the *AtbZIP9* cDNA under the control of CaMV 35S promoter (35S-*AtbZIP9*), in a T-DNA *knockout* null mutant (*atbzip9-1*) and in the wild type (WT). (C) Growth and development and (D) vascular cylinder anatomy were compared in the different genotypes and no detectable phenotypic differences were observed between them. Ph: phloem; Xy: xylem. Scale bar represents 4 μM.

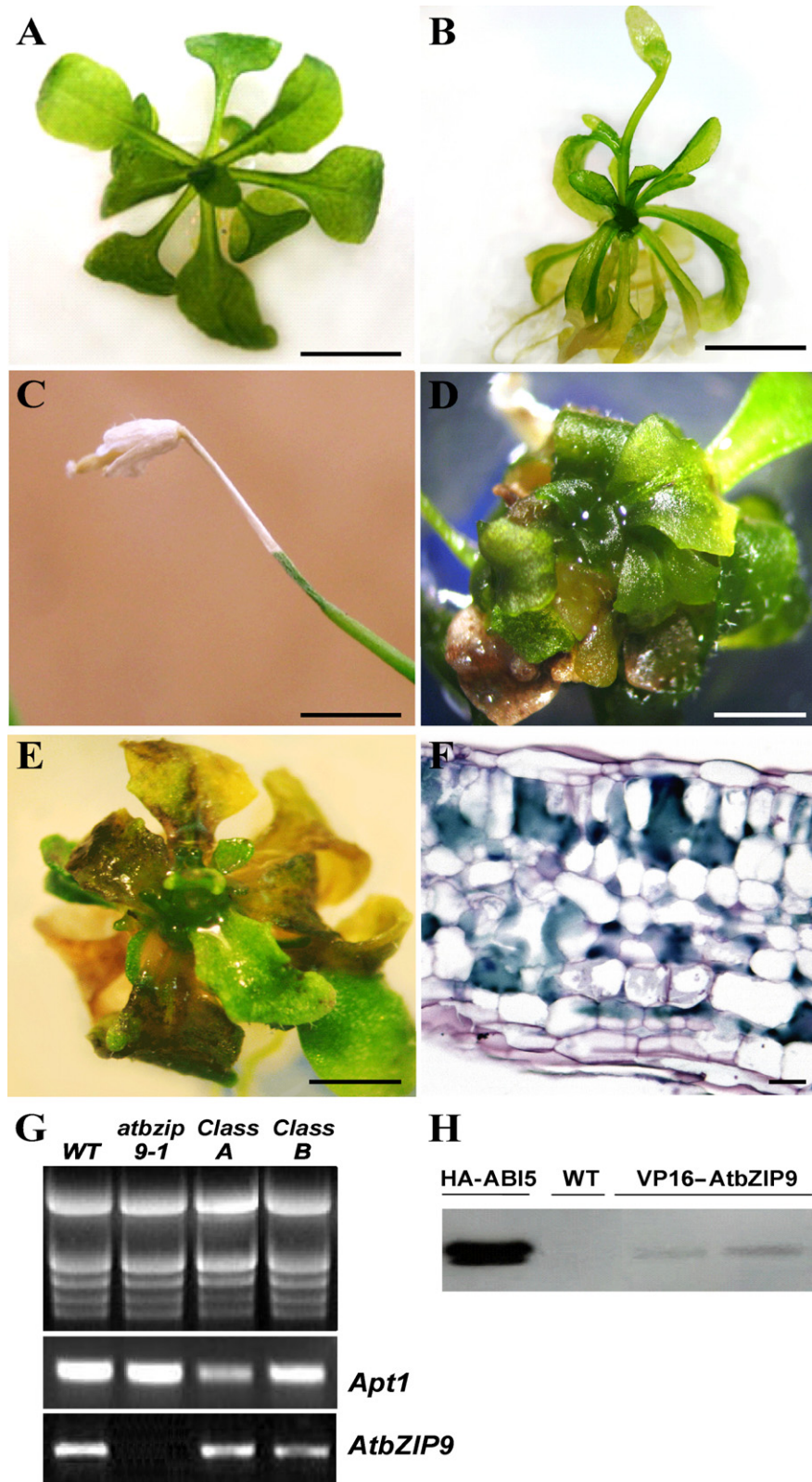


Fig. 4. Characterization of a constitutive activator allele of *AtbZIP9* (VP16-*AtbZIP9*). (A) Wild-type plant 15 days after germination. (B-F) Phenotypic alterations of VP16-*AtbZIP9* transgenic plants. (B) Representative plant of Class A primary transformants which has been grown for 25 days after germination. (C) Dried inflorescence of a class A transformant. (D and E) Representative plants of Class B primary transformants which have been grown for 25 days after germination. (F) Transversal section of Class B leaf stained with toluidine blue showing increased phenolic compound (green colour) deposition within and between cells. Scale bars: A and B: 0.6 cm; C and D: 2 mm; F: 80 μ m. G. Semi-quantitative RT-PCR analysis of VP16-*AtbZIP9* expression in plants grown for 30 days after germination. These plants were cultivated on solid half-strength Murashine and Skoog medium (MS/2) with 0.5% (w/v) sucrose. (H) Detection of HA-VP16-ATBZIP9 fusion protein by Western blot. A transgenic line expressing a fusion between the hemagglutinin tag and the cDNA sequence of *ABI5* gene (HA-ABI5) was used as a positive control.

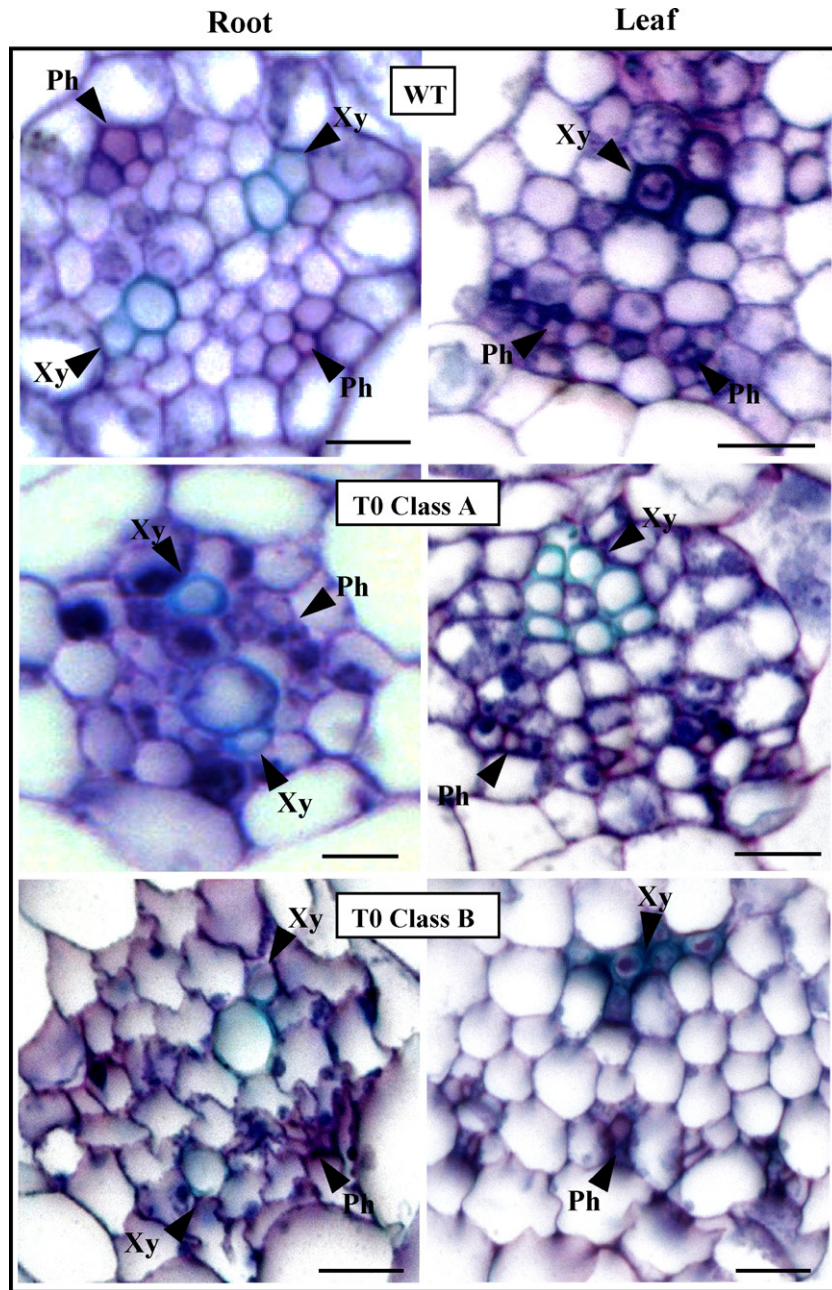


Fig. 5. Comparative analysis of root and leaf vascular anatomy in transformed (T0) VP16-*AtbZIP9* and wild-type plants. Roots and leaves of both T0 classes show vascular cylinder disorganization. Phloem cells can hardly be visualized and their possible locations are indicated. Ph: phloem; Xy: xylem. Scale bars: 30 μ M.

AtbZIP9, we generated Arabidopsis transgenic plants for a fusion between *AtbZIP9* cDNA and the strong activation domain from the *Herpes simplex* virus VP16 protein, which is expressed from the native *AtbZIP9* promoter sequence. Potentially, this new allele, named VP16-*AtbZIP9*, could constitutively activate *AtbZIP9* target genes and possibly induce developmental and/or physiological changes which may be relevant to uncover some aspect of *AtbZIP9* function. To avoid any interference with the wild-type allele we transformed

the *atbzip9-1* T-DNA insertion null mutant. From 400 *in vitro* grown VP16-*AtbZIP9* primary transformants (T0), 280 (70%) displayed clear phenotypic modifications late in development, approximately after 8/10 leaves had emerged. We were unable to propagate these phenotypically altered T0 plants since they did not grow further after transplantation to soil. Phenotypic modifications essentially concerned leaf development and could be divided in two main classes. The first class (Class A, 20% (80) of the T0 plants), typically showed elongated and

Wild type (WT) and VP16-*AtbZIP9* plants were grown on solid MS/2 with 0.5% (w/v) sucrose for 15 days while HA-ABI5 were grown on liquid MS-2 with 0.5% (w/v) sucrose for 2 days after germination. Fusion proteins were detected with an antibody against the HA tag from 20 μ g of total protein in the case of HA-ABI5, 25 μ g (left) and 30 μ g (right) for VP16-*AtbZIP9*. Expected sizes are 51 kDa for HA-ABI5 and 46 kDa for HA-VP16-ATBZIP9.

slightly chlorotic leaves with upward curling margins as compared to the wild type (Fig. 4A and B). Under *in vitro* sterile conditions, this class of T0 plants also produced inflorescences whose tips dried out before silique formation (Fig. 4C). The second class of phenotypic modifications (Class B, 50% (2 0 0) of the T0 plants) was characterized by atrophied plants that produced small and morphologically altered leaves when compared to the wild type (Fig. 4A, D and E). Leaf shape alterations ranged from deviations of wild-type morphology (elongated, heart-shaped, serrated and recorted) to highly deformed (Fig. 4D and E and data not shown). Most of these plants remained in the vegetative stage and did not produced inflorescences. In the leaves of this class of T0 plants, accumulation of brownish compounds and necrotic lesions were frequently observed (Fig. 4E). Leaf section treated with toluidine blue resulted in green staining (Fig. 4F) which suggest that the brownish compounds are phenolic metabolites [24]. This was further confirmed by black staining induced by ferric chloride treatment (data not shown [24]). These phenolic compounds accumulate within the cells as well as in the intracellular space (Fig. 4F). This accumulation may represent profound alterations in phenolic compound production and targeting in response to some physiological stress condition. Phenolic compounds have been shown to play an important role in resistance to biotic and abiotic stresses [25], to serve as signaling molecules [26], and to modulate the action of auxins [27]. None of the plants showed obvious root growth modifications. Analysis of RNA extracted from a representative sample of about 20 T0 plants of each of these two classes showed that the VP16-AtbZIP9 construct was expressed (Fig. 4G). Although we were able to detect the expression of the adenosine phosphoribosyl transferase control gene (*AptI*) in the two classes of T0 plants, considering the drastic developmental alterations of these plants, further detailed analysis should be performed to establish any precise correlation between phenotypic changes observed and the level of VP16-AtbZIP9 expression. We also verified that the VP16-AtbZIP9 construct was functional since the HA::VP16::AtbZIP9 fusion protein was detected in a total protein extract obtained from a F1 population resulting from selfing of a T0 transformant which did not present any clear phenotypic alterations (Fig. 4H). The fact that control T0 plants for the VP16 activator domain expressed under the control of the strong CaMV 35S promoter did not cause any of the changes observed in the T0 VP16-AtbZIP9 plants ruled out the possibility of non-specific VP16 effects such as squelching. We therefore conclude that the observed changes on leaf development are related to the expression of the VP16-AtbZIP9 construct.

Since the *AtbZIP9* promoter regulatory sequences were found to dictate expression in the phloem, we anticipated that some alteration of phloem development might have occurred in T0 plants of both A and B classes. A comparative analysis of leaf and root cross sections was therefore carried out. The relative position of xylem and phloem within the vascular tissues was found to be similar between the T0 plants of the two classes and the wild type, with a diarch and abaxial/adaxial

pattern in root and leaf vasculature, respectively (Fig. 5). However, in class A and B plants, phloem cells were difficult to identify in leaf bundles and could hardly be detected at all in roots of these two classes of T0 plants when compared to the wild type (Fig. 5) possibly reflecting some alteration of phloem formation and phloem differentiation. Besides, we noticed that in Class B plants, the parenchyma layer in leaf vasculature was significantly more developed than in class A and wild-type genotypes (Fig. 5). Finally, in root vascular cylinder, cell shape was irregular and the cell arrangement was disordered indicating a possible alteration of the cell division pattern and cell wall formation (Fig. 5). It appears therefore, that the VP16-AtbZIP9 construct caused defects in the vascular development which was most clearly detected in the root. Despite of this problem, the apparent lack of a root growth defect *in vitro* may simply be explained by the nutrient-rich medium (MS/2 including sucrose) used to cultivate the T0 individuals and could help explain our inability to grow the T0 plants in soil. We suspect that the developmental modifications observed in the T0 plants may be a consequence of changes in vascular tissue's functional properties. Long distance transport through the xylem and phloem of nutritional resources, hormones, or macromolecular regulatory signals (RNAs and proteins) play an important role in the regulation of plant development [28]. The identification of *AtbZIP9* target genes will be essential to integrate *AtbZIP9* in the regulatory network of phloem development.

Acknowledgements

We thank V. Pautot and H. Morin (Cellular Biology Lab, INRA-Versailles, France) for assistance during the development of *in situ* mRNA localization, F. Parcy (Laboratoire de physiologie cellulaire végétale UMR5168 17, Grenoble, France) for providing PFP100, PFP101HAVP16 vectors and Arabidopsis transgenic lines expressing the 35S::HA::ABI5 and J.L. Argueso for English corrections (Departamento de Genética e Evolução-IB, Unicamp). This work was supported by FAPESP (Fundação de Amparo a Pesquisa do Estado de São Paulo) and CAPES (Coordenação de Aperfeiçoamento de Pessoal de Nível Superior).

References

- [1] M. Jakoby, B. Weisshaar, W. Droge-Laser, J. Vicente-Carbajosa, J. Tiedemann, T. Kroj, F. Parcy, bZIP transcription factors in Arabidopsis, *Trends Plant Sci.* 7 (2002) 106–111.
- [2] M. Vincentz, C. Bandeira-Kobarg, L. Gauer, P. Schlogl, A. Leite, Evolutionary pattern of angiosperm bZIP factors homologous to the maize Opaque2 regulatory protein, *J. Mol. Evol.* 56 (2003) 105–116.
- [3] P. Ciceri, F. Locatelli, A. Genga, A. Viotti, R.J. Schmidt, The activity of the maize Opaque2 transcriptional activator is regulated diurnally, *Plant Physiol.* 121 (1999) 1321–1328.
- [4] B.G. Hunter, M.K. Beatty, G.W. Singletary, B.R. Hamaker, B.P. Dilkes, B.A. Larkins, R. Jung, Maize opaque endosperm mutations create extensive changes in patterns of gene expression, *Plant Cell* 14 (2002) 2591–2612.
- [5] P. Lara, L. Ónate-Sánchez, Z. Abraham, C. Ferrándiz, I. Díaz, P. Carbonero, J. Vicente-Carbajosa, Synergistic activation of seed storage protein

- gene expression in Arabidopsis by ABI3 and two bZIPs related to Opaque2, *J. Biol. Chem.* 278 (2003) 21003–21011.
- [6] H. Kaminaka, C. Näke, P. Eppele, J. Dittgen, K. Schütze, C. Chaban, B.F. Holt III, T. Merkle, E. Schäfer, K. Harter, J.L. Dangl, bZIP10-LSD1 antagonism modulates basal defense and cell death in Arabidopsis following infection, *EMBO J.* 25 (2006) 4400–4411.
- [7] T. Heinekamp, A. Strathmann, M. Kuhlmann, M. Froissard, A. Müller, C. Perrot-Rechenmann, W. Droge-Laser, The tobacco bZIP transcription factor BZI-1 binds the GH3 promoter in vivo and modulates auxin-induced transcription, *Plant J.* 38 (2004) 298–309.
- [8] M. Kuhlmann, K. Horvay, A. Strathmann, T. Heinekamp, U. Fischer, S. Bottner, W. Droge-Laser, The alpha-helical D1 domain of the tobacco bZIP transcription factor BZI-1 interacts with the ankyrin-repeat protein ANK1 and is important for BZI-1 function, both in auxin signaling and pathogen response, *J. Biol. Chem.* 278 (2003) 8786–8794.
- [9] F. Weltmeier, A. Ehlert, C.S. Mayer, K. Dietrich, X. Wang, K. Schütze, R. Alonso, K. Harter, J. Vicente-Carbajosa, W. Droge-Laser, Combinatorial control of Arabidopsis proline dehydrogenase transcription by specific heterodimerisation of bZIP transcription factors, *EMBO J.* 25 (2006) 3133–3143.
- [10] A. Ehlert, F. Weltmeier, X. Wang, C.S. Mayer, S. Smeekens, J. Vicente-Carbajosa, W. Droge-Laser, Two-hybrid protein–protein interaction analysis in Arabidopsis protoplasts: establishment of a heterodimerization map of group C and group S bZIP transcription factors, *Plant J.* 46 (2006) 890–900.
- [11] T. Murashige, F. Skoog, A revised medium for rapid growth and bio-assays with tobacco tissue cultures, *Physiol. Plant* 15 (1962) 473–497.
- [12] A. Sessions, E. Burke, G. Presting, G. Aux, J. McElver, D. Patton, B. Dietrich, P. Ho, J. Bacwaden, C. Ko, J.D. Clarke, D. Cotton, D. Bullis, J. Snell, T. Miguel, D. Hutchison, B. Kimmerly, T. Mitzel, F. Katagiri, J. Glazebrook, M. Law, S.A. Goff, A high-throughput Arabidopsis reverse genetics system, *Plant Cell* 14 (2002) 2985–2994.
- [13] S. Bensmihen, A. To, G. Lambert, T. Kroj, J. Giraudat, F. Parcy, Analysis of an activated *ABI5* allele using a new selection method for transgenic *Arabidopsis* seeds, *FEBS Lett.* 561 (2004) 127–131.
- [14] R.A. Jefferson, Assaying chimeric genes in plants: the GUS fusion system, *Plant Mol. Biol. Rep.* 5 (1987) 387–405.
- [15] C. Yanisch-Perron, J. Vieira, J. Messing, Improved M13 phage cloning vectors and host strains: nucleotide sequences of the M13mp18 and pUC19 vectors, *Gene* 33 (1985) 103–119.
- [16] R. Topfer, V. Matzeit, B. Gronenborn, J. Schell, H.H. Steinbiss, A set of plant expression vectors for transcriptional and translational fusions, *Nucleic Acids Res.* 15 (1987) 5890.
- [17] J.M. Short, J.M. Fernandez, J.A. Sorge, W.D. Huse, Lambda ZAP: a bacteriophage lambda expression vector with in vivo excision properties, *Nucleic Acids Res.* 16 (1988) 7583–7600.
- [18] N. Bechtold, J. Ellis, G. Pelletier, In planta Agrobacterium-mediated gene transfer by infiltration of adult Arabidopsis thaliana plants, *C. R. Acad. Sci. Paris, Life Sci.* 316 (1993) 1194–1199.
- [19] C. Koncz, J. Schell, The promoter TL-DNA gene 5 controls the tissue-specific expression of chimaeric genes carried by a novel type of Agrobacterium vector, *Mol. Genet.* 204 (1986) 383–396.
- [20] J. Logemann, J. Schell, L. Willmitzer, Improved method for the isolation of RNA from plant tissues, *Anal. Biochem.* 163 (1987) 16–20.
- [21] C. Zhao, J.C. Craig, H.E. Petzold, A.W. Dickerman, E.P. Beers, The Xylem and Phloem transcriptomes from secondary tissues of the Arabidopsis root-hypocotyl, *Plant Physiol.* 138 (2005) 803–818.
- [22] J.Y. Lee, J. Colinas, J.Y. Wang, D. Mace, U. Ohler, P.N. Benfey, Transcriptional and posttranscriptional regulation of transcription factor expression in Arabidopsis roots, *Proc. Natl. Acad. Sci. U.S.A.* 103 (2006) 6055–6060.
- [23] J.Z. Zhang, Overexpression analysis of plant transcription factors, *Curr. Opin. Plant Biol.* 6 (2003) 430–440.
- [24] M. Ling-Lee, G.A. Chilvers, A.E. Ashford, A histochemical study of phenolic materials in mycorrhizal and uninfected roots of eucalyptus fastigata Deane and Maiden, *New Phytologist* 78 (1977) 313–328.
- [25] E. Siranidou, Z. Kang, H. Buchnauer, Studies on symptom development, phenolic compounds and morphological defense responses in wheat cultivars differing in resistance to Fusarium Head blight, *J. Phytopathol.* 150 (2002) 200–208.
- [26] R.A. Dixon, N.L. Paiva, Stress-induced phenylpropanoid metabolism, *Plant Cell* 7 (1995) 1085–1097.
- [27] R. Volpert, W. Osswald, E.F. Elstner, Effects of cinnamic acid derivatives on indole acetic acid oxidation by peroxidase, *Phytochemistry* 38 (1995) 19–22.
- [28] T.J. Lough, W.J. Lucas, Integrative plant biology: role of phloem long-distance macromolecular trafficking, *Annu. Rev. Plant Biol.* 57 (2006) 203–232.